

# Microgel containers for self-healing polymeric materials: morphology prediction and mechanism of formation

Alexandra Latnikova<sup>1\*</sup>, Dmitry Grigoriev<sup>2\*</sup>, Helmuth Möhwald<sup>2</sup>, Dmitry Shchukin<sup>3</sup>

<sup>1</sup>Fraunhofer Institute for Applied Polymer Research IAP, Geiselbergstraße 69, 14476 Potsdam, Germany

<sup>2</sup>Max Planck Institute of Colloids and Interfaces, Am Muehlenberg, 14476 Potsdam, Germany

<sup>3</sup>University of Liverpool, Crown Street, Liverpool L69 7ZD, United Kingdom

*Keywords: microgel, microparticles, encapsulation, morphology, coreshell, compact, multicompartment, interfacial polymerization*

## Abstract

18 types of gel microparticles, composed of 3 polymer types and 6 different solvents, were prepared by interfacial polymerization and compared in a systematic way with respect to their structure and function. Three types of morphologies, specific for each polymer-solvent pair, were observed: core-shell, multicompartment and compact. The morphology was found to be a direct consequence of the specific polymer-solvent interactions and can be, in most cases, predicted on the basis of simple swelling experiments with a chosen polymer in the solvent. Further, the Hansen Solubility Parameters approach was applied to the investigated systems enabling a reliable morphology prediction of microgel particles made of any polymer/solvent combination with known solubility parameters (spheres). The mechanisms responsible for the formation of particles with different morphologies are also discussed.

## Introduction

Development of new self-healing materials able, upon damage, to recover their integrity and other properties autonomously is one of most rapidly growing fields in modern materials engineering [1 – 5]. Depending on that whether self-healing is an inherent latent property of the material matrix or is artificially imparted to this, these can be divided into two subclasses, so-called “intrinsic” or “extrinsic” self-healing materials [1, 2, 4, 5], respectively. For the latter, the self-healing ability of the entire material is determined by the objects of external origin embedded in the material matrix, such as microcontainers, microcapsules, etc. The cargo of these components is mobile and reactive and can, therefore, recover the material integrity upon damage. In spite of several advantages of intrinsic self-healing materials (no additional healing agent needed, multiple healing events are possible etc.) their applicability

\*Corresponding authors: [alexandra.latnikova@iap.fraunhofer.de](mailto:alexandra.latnikova@iap.fraunhofer.de);  
[dmitry.grigoriev@mpikg.mpg.de](mailto:dmitry.grigoriev@mpikg.mpg.de)

depends strongly on the type of materials to be healed as well as on the specific healing scheme and is, therefore, not always feasible [5].

Extrinsic self-healing materials may be further classified into two different groups in accordance with their inner structure. If the components containing the healing agents are discretely distributed in the material matrix, one speaks about capsules-based self-healing materials. In case of a continuous system of capillaries or channels filled with the healing agent and incorporated into the matrix, the term “vascular” self-healing materials is commonly used [4, 5].

Successful practical application of vascular self-healing materials is almost completely restricted to the use of hollow glass fibers of relatively large size filled with a healing agent and forming a 1D network inside the material matrix [6]. Advanced methods for producing vasculature of higher connectivity within the matrix of self-healing materials involve the use of fugitive inks for direct-ink printing of the 3D scaffold with its subsequent removal leading to 3D channel networks [7, 8] or utilization of sacrificial melt-spun sugar fibers [9]. These systems and methods are, however, still far from implementation into self-healing materials of practical relevance.

On the other hand, extrinsic self-healing materials based on the embedding of micro- or nanocapsules in the material matrix are most established now since the preparation and following incorporation of their healing components (capsules) is relatively simple, economic and can be realized in very different ways depending on the capsules size, their specific chemical composition, opening triggers etc.

An approach to creation of extrinsic capsules-based self-healing materials was proposed more than two decades ago [10, 11]. Initially restricted only to polymeric bulk materials [11, 12] it was further not only significantly optimized [13 – 18] for these applications but also transferred to the 2D case yielding a novel class of polymeric coatings – self-healing coatings [19 – 24].

The healing capacity of capsules-based self-healing materials is related to the amount of healing agent enclosed in the capsules. This parameter, in turn, depends on the capsule volume fraction and on their “usable” volume, i.e. on their morphology. In case of a constant physically reasonable volume fraction, an optimal capsule morphology providing a maximal amount of healing agent is the core-shell morphology with the lowest shell thickness still ensuring the mechanical stability of capsules.

For the preparation of capsules especially on a micro- or nanoscale, an emulsion route is frequently used [18, 23, 25-33]. With this approach, the droplets of dispersed phase of an

emulsion undergo an interfacial polymerization reaction such as polyaddition or polycondensation leading to the formation of polymeric network in the capsules shell or in the entire volume of micro- or nanoobjects yielding the compact particles.

Usage of cross-linked polymers as microparticle matrix material is often advantageous compared to the linear analogs, because of the superior mechanical properties, lower permeability coefficients and chemical stability of the former. Any plurality of microparticles consisting of cross-linked polymer enclosing a liquid can be considered as microgel. Depending on the specific self-healing application, microgels should be designed to possess certain properties such as chemical stability, release properties, surface chemistry, etc. All of these properties are mainly determined [26-28, 30, 32] by the microgel morphology and by the relationship between physicochemical properties of a polymer and an agent to be encapsulated.

Because of practical importance of polymer micro- and nanoparticles of different morphology used nowadays in many industry branches for several decades it is important to investigate the fundamental aspects allowing the prediction and control of the properties of these objects and, first of all, their morphology. For the microcapsules, Sliwka [26] tried to develop such a descriptive approach on the basis of semi-quantitative use of Hildebrand solubility parameter.

In the last decade, Landfester, Crespy and co-workers carried out several comprehensive studies [27-32, 35] where various aspects related to the preparation of nano- and microcapsules on the emulsion basis and to their final morphology (core-shell, compact etc.) were investigated. Influence of numerous physicochemical parameters such as concentrations and hydrophobicity of solvent and polymer components in the dispersed “oil” phase [27, 28, 30, 32]; rate of the reactants addition during interfacial polycondensation reaction [27]; nature of copolymers [28] and surfactants (interfacial tension) used for the emulsification [28, 29]; inversion of polar/apolar continuous vs. dispersed phases [30]; temperature [28-30] on the formation, properties and morphology of capsules were analyzed. Most of these considerations were done on the qualitative or semi-quantitative level [28, 30, 31] using the classical approaches such as Flory–Huggins [28, 31] or Hildebrand [30] solubility parameters.

The quantitative application of modern and more versatile Hansen solubility parameters (HSP) approach to several two-component polymer-solvent systems was recently made by Latnikova in her PhD thesis [33]. Part of these results was subsequently reported showing the possibility to predict the morphology of microcapsules loaded with a certain

liquid corrosion inhibitor acting as a solvent [34]. Very recently, Landfester and colleagues [35] demonstrated the quantitative use of HSP for the encapsulation of highly volatile fragrance-like liquids and for the prediction of their encapsulation efficiency. Unfortunately, the systematic quantitative analysis performed in Ref. [33] on the HSP basis for the array of 18 binary polymer-solvent systems remained almost unrecognized by other scientists. In this connection, the work at hand is a concentrated and rearranged version of [33] in order to disseminate the main results reported there to the broader scientific community.

Herein, we will examine the simplest case of two-component polymer/solvent microparticles prepared by interfacial polymerization. We will make an attempt to answer some essential questions considering formation of particles consisting of a cross-linked polymer and a liquid component, e.g.:

1. What kind of morphologies can be generally expected?
2. Which factors influence the morphology?
3. What are mechanisms leading to the formation of particles of various morphologies?

For this purpose, we have chosen three types of cross-linked polymers and six solvents with considerably different solvency, resulting in 18 polymer/solvent combinations. The microgels were prepared by interfacial polymerization (polyaddition and polycondensation). The morphology of each microgel type (corresponding to polymer/solvent combination) was investigated and found to be directly related to the interaction parameter for each polymer-solvent pair estimated on the basis of swelling experiments and Hansen Solubility Parameters approach. Based on that, we suggest possible mechanisms that would explain formation of microparticles with the broad spectrum of morphologies, including core-shell, inverse core-shell, multicompartiment and compact.

## Materials

Poly[(phenyl isocyanate)-co-formaldehyde] (isocyanate prepolymer, number of reactive groups per molecule  $\sim 3.0$ , MW $\sim 375$ ), terephthaloyl chloride (TPhCl), glycerol, ethylenediamine (EDA), tetraethylenepentamine (TEPA), poly(vinyl alcohol) (PVA, MW $\sim 9,000-10,000$ , 80% hydrolyzed), 1,4-diazabicyclo[2.2.2]octane (DABCO), ethanol (EtOH), methanol (MeOH), acetone, toluene, chloroform, cyclohexanone (CHn), dimethyl phthalate (DMPh), diethyl phthalate (DEPh), dioctyl phthalate (DOPh), 4-methoxybenzaldehyde (anisaldehyde), tetrahydrofuran (THF), styrene, N-methyl-2-pyrrolidone, dimethyl sulfoxide, 1-dodecanethiol, 2,2,2-trifluoro ethanol, 1-hexanol, diaminocyclohexane, dibutyl phosphate (DBuPh). All chemicals were of reagent grade (at

least 98.5 wt% purity), were purchased from Sigma–Aldrich and used without further purification. The Millipore Milli-Q Plus 185 water was used in all experiments.

## Methods

### Preparation of particles

Microparticles of polyurethane (PU), polyurea (PUa) and polyamide (PA) were prepared by interfacial polymerization. Fig. 1 shows the principal chemical reactions responsible for the PU, PUa and PA linkage formation. The particle preparation always started with the preparation of oil-in-water (O/W) emulsion; emulsion droplets are believed to act as the soft templates for forming solid microparticles. The dispersed phase contained water-insoluble reactive monomer and one of the chosen solvents. Continuous aqueous phase contained emulsion stabilizer and the second reactive monomer. Both, continuous and dispersed phase were clear true solutions. Formation of polymer was due to the reaction between two complementary reactive monomers on the interface between two immiscible phases.

Six water-immiscible solvents of different polarity were chosen as model entrapped liquid materials: toluene (Tol), chloroform (Chl), cyclohexanone (CHn), dimethyl phthalate (DMPH), diethyl phthalate (DEPh) and dioctyl phthalate (DOPh). In such a manner, 18 (3 polymers×6 solvents) different polymer-solvent combinations were realized.

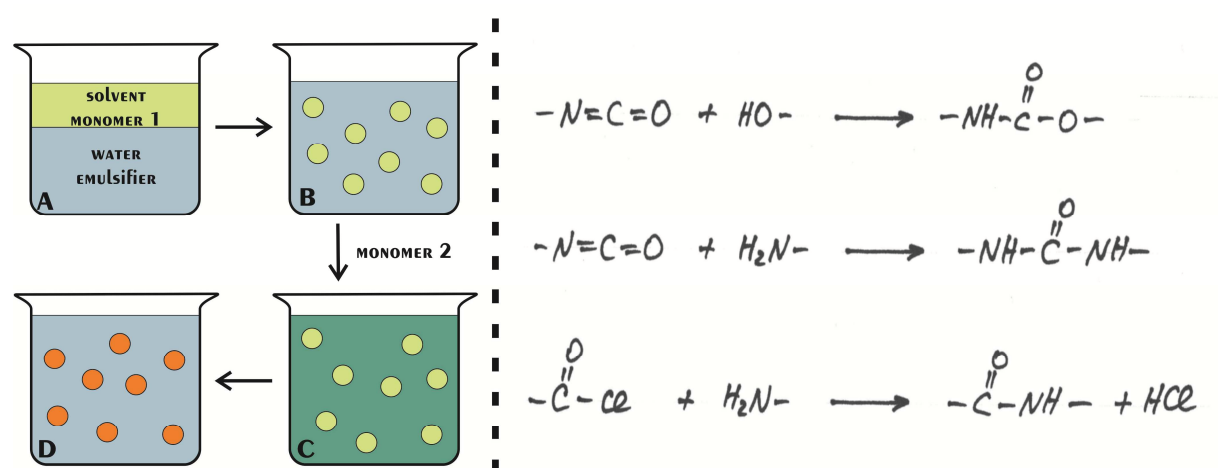


**Fig.1.** Left: Schematic representation of the interfacial polymerization process: two immiscible phases (A), emulsion formation (B), Second reactive monomer addition (C), monomer consumption leading to polymer particles formation (D). Right: Chemical reactions corresponding to the formation of urethane, urea and amide linkage.

The oil phase of the initial O/W emulsions in cases of PU and PUa microparticles was prepared by the dissolution of isocyanate prepolymer (300 mg) in 0.70 ml of one of above mentioned solvents. In case of PA microparticles, the same amount of TPhCl was used. The

corresponding oil phase was then emulsified in 10 ml of 2 wt% aqueous PVA solution saturated with corresponding solvent for 3 minutes at 16000 rpm using an ULTRA-TURRAX® high-speed homogenizer (IKA® Werke, Staufen, Germany).

For the preparation of PU microparticles, a solution of glycerin (4 ml) and DABCO (200 mg) in water (6 ml) was added slowly to the emulsion. This mixture was left for one hour at 65°C under stirring. Then, heating was stopped and the system was left without stirring overnight. A suspension of particles was dialyzed in order to remove the residual glycerol. For this purpose a membrane with the pore size of 12-18 kDa was utilized. Further, the particles were washed 3 times with water by centrifugation followed by re-dispersion in pure water by hand-shaking. Finally, the precipitate was separated by decantation and dried at normal conditions overnight. Preliminary dialysis was necessary to enable the particle separation by centrifugation, since the density of the glycerol-containing aqueous phase was close to the density of the resulting microparticles. Heating and addition of DABCO as polymerization reaction catalyst are necessary in order to achieve reasonable polymerization times of PU due to the comparatively low reactivity of isocyanates towards alcohols.

For the preparation of PUa microparticles, a mixture of EDA (1.1g) and TEPA (2.8 g) was used as the water-soluble reactive monomer. This mixture was dissolved in 10 ml of water saturated with corresponding solvent and added slowly to the emulsion under stirring without heating. After 10 minutes stirring was stopped, and the mixture was left for reaction completion overnight. Further, the particles were washed and dried in the same manner as described above for the PU microparticles.

For the preparation of PA microparticles, an aqueous solution of the same amines (0.91 g and 3.4 g, respectively) was employed as water-soluble reactive monomer. The mixture of amines was dissolved in 10 ml of water saturated with corresponding solvent and added slowly to the corresponding emulsion under stirring without heating. After 10 minutes, stirring was stopped and the mixture was left for the reaction completion overnight. Finally, the particles were washed and dried in the same fashion as for the PU and PUa microparticles.

Pure PU and PUa polymers without solvent were synthesized in the same manner as solvent-containing particles with the only isocyanate prepolymer as an oil phase (it is liquid at room temperature). For PA, this approach could not be applied, since TPhCl is a solid substance. The synthesis of PA polymer was performed on the planar toluene-water interface. TPhCl was dissolved in toluene; amine mixture was dissolved in Milli-Q water. In the latter synthesis, the composition and the ratio of the aqueous and oil phases were the same as for the PA microparticle synthesis. The film forming between the two phases was collected.

## Characterization

### *Scanning electron microscopy (SEM)*

For the characterization of the resulting particles by SEM, a small amount (10  $\mu\text{l}$ ) of the particle suspension was placed on the sample holder and left overnight to dry at atmospheric pressure. If needed, the resulting sample was crushed with a razor blade. An alternative procedure was applied in case the particles could not be crushed as powder (PUa-CHCl<sub>3</sub>). For that, particles were introduced into the polymeric (epoxy) matrix and after matrix curing thin slices (not thicker than 1 mm) were cut and arranged on the sample holder in such a way, that the cut edge of the sample would be nearly parallel to the sample holder surface. (SEM) measurements were performed using a Gemini 1550 instrument at an operation voltage of 3 keV. All samples were gold-sputtered.

### *Dynamic light scattering (DLS)*

A Zeta Sizer Nano ZS (Malvern Instruments, UK) was utilized to determine the size distribution of the microparticles. Before the measurement all samples were appropriately diluted to obtain slightly turbid dispersions. At least three measurements of 15 runs each were averaged.

### *Swelling behavior of polymers*

To determine the extent of swelling, 200 mg of pure PU, PUa or PA powder was dispersed in 2 ml of each solvent. After one week of shaking, the dispersion was centrifuged in order to separate the swollen polymer grains. After removal of the residual solvent, the amount of solvent absorbed by each polymer was calculated as the mass difference between swollen and initial particles.

### *Hansen Solubility Parameters (HSP) approach*

HSP approach [36-40] is a phenomenological extension of the Hildebrand approach primarily used for polymer-liquid systems, to systems with high extent of polar and hydrogen bond interactions. The Hildebrand solubility parameter ( $\delta$ ) provides a numerical estimate of the degree of interaction between materials, and can be a good indication of solubility. Materials with similar values of  $\delta$  are likely to be miscible. In Hansen's approach the  $\delta$  parameter is considered to be a combination of dispersion  $\delta_D$ , polar  $\delta_P$  and hydrogen-bonding  $\delta_H$  components, which are related by:

$$\delta^2 = \delta_D^2 + \delta_P^2 + \delta_H^2 \quad (1)$$

The essential improvement of the HSP approach compared to the Hildebrand's one is that in the former one all three parameters should simultaneously "fit", making Hansen's approach much more precise in prediction of polymer swelling/solubility behavior [40].

For the practical procedure, a three-dimensional graph is plotted in the coordinate system with  $\delta_D$ ,  $\delta_P$  and  $\delta_H$  as the orthogonal axes. A point on the graph represents a chosen low molecular substance with corresponding values of HSP. For polymers, solubility spheres instead of points are traditionally used. To construct the HSP sphere for a given polymer, the sphere should be located on a graph in such a way that the "good" solvents for this polymer are located inside the sphere, while the "poor" ones are located outside. Both the location of the sphere center and the sphere radius should be fitted. The resulting three-dimensional graph is hard to present, therefore for polymers very often only the  $\delta_H(\delta_P)$  projection is used, since it is considered that the specific interactions are mainly responsible for the polymer phase behavior. Here, only the  $\delta_H(\delta_P)$  projection of the 3-D HSP graph is also presented. The other two projections ( $\delta_H(\delta_D)$  and  $\delta_P(\delta_D)$ ) are in agreement with the one presented here. It is important to underline that "good" and "poor" quality of a chosen solvent in Hansen's approach is not related to the classical Flory's approach. The border between "good" and "poor" solvent in Hansen's approach can be conditionally chosen by the "user" according to the context or application. This approach suffers from the lack of thermodynamic "exactness", but offers other advantages being more user-friendly and application-oriented.

## Results and discussion

Eighteen types of microparticles were prepared after the washing and drying procedures in the form of powders. Already from the appearance of the resulting powders one could guess if the solvents were entrapped/encapsulated with different success. Some powders were free-flowing, while others were sticky. The re-dispersion of the sticky powder in water was sometimes problematic, while re-dispersion of the free-flowing ones was effortless. The stickiness of the resulting powder was attributed to the partial leakage of an encapsulated solvent leading to the appearance of capillary forces holding the particles together in the aqueous medium. The size of the synthesized microparticles was estimated by observation of particle suspensions by optical and electron microscopy. All batches had similar broad size distribution between 2 and 20  $\mu\text{m}$ . This was expected, since the main factors determining the emulsion droplet size (stirring speed, oil phase content and stabilizer concentration) in each batch were equal. At the same time, the size of the initial emulsion oil droplets determines (and is later almost equal to) the size of the resulting polymeric particles [41, 42]. Some

samples were additionally investigated by DLS, the results were in agreement with optical microscopy observations. The size distribution of the particles was very broad and bimodal – there were two populations of particles: with the average size of 1  $\mu\text{m}$  and 8  $\mu\text{m}$ . Broad size distribution of the emulsion droplets and, consequently, of the resulting microparticles is common, when mechanical stirring is used. Addition of a superhydrophobe (like hexadecane etc.) might have helped to decrease the polydispersity, but would significantly complicate the morphology analysis, since the system would have a third component. Therefore, no attempts to increase the monodispersity by changing the composition were made. The morphology of particles was assumed to be independent of the particle size, at least in the micron-submicron region.

The qualitative analysis of the particle shape and surface topography was performed on the basis of SEM images (Fig.1 SI). Depending on the polymer-solvent combination, different particle shapes were observed: spherical, spheroidal with concavities and/or folds and collapsed. Appearance of small concavities could be a result of particle collision upon the first steps of the polymerization reaction when the particle shells are still soft. This would not, however, explain the fact that some particles did have the concavities, while others did not. Folding and even collapse of particles could be explained by the high vacuum used in SEM, leading to the evaporation of the solvent or partial extraction of the particle liquid content during the washing procedure. However, observation of the particles under the optical microscope just before the washing step showed (the data are not presented) that concavities and folds appeared before vacuum, washing and drying procedures have been carried out. This means that the appearance of a certain extent of roughness on the surface of some particles has an intrinsic character and is only determined by polymer-solvent pair interactions. We assume that irregular compression or shrinkage of the polymer during cross-linking can be responsible for the rough surface or irregular shape of the particles. Local fluctuations of the interfacial tension at the surface of a semi-liquid particle shell can be also a reason.

If there was no or a very small amount of liquid material left inside the particle (the case for all polyamide particles apart from the toluene-containing ones), the particles were considered as “collapsed”. For such particles further morphological analysis is not necessary, since the core-shell morphology can be concluded from the particle appearance (if the rests of the particle walls can be distinguished). Spherical, bumped and folded particles should be analyzed further in more details in order to find out, how the polymer material is distributed inside the particle.

Each type of particles was synthesized at least three times. The shape of the PU and PUa particles was reproducible, only slight variation of the shape from batch to batch was observed (mainly, in the size and number of concavities and folds).

The shape of the PA particles varied significantly from batch to batch. Some particles had generally spherical shape (as in the case of toluene-containing ones), while some were collapsed (as for other solvents). In one batch, particles were either mainly spherical or collapsed. This effect was not solvent-specific; both types of particles were observed for most solvents in different batches. The shape was found to be influenced by the drying procedure. Freeze-dried particles exhibit spherical shape more often than those dried in air, though not always. The effect of the drying procedure on the final shape of PA microparticles/capsules was already discussed in the literature [43]. The phenomenon can be explained by the plasticizing effect of water on PA. In an aqueous medium, the walls of particles are soft and elastic due to the swelling of the polymer in water. Strong mechanical impact experienced by the microobjects during drying due to capillary forces leads to their collapse. Freeze-drying helps to preserve the spherical shape during drying. This hypothesis is supported by the fact that in the suspension most of the PA particles have spherical shape with minor amount of concavities or folds. Although further examination of the parameters influencing mechanical properties of the PA particles might be very useful for their further application, it was not performed here. The main goal here was to investigate the morphology. Appearance of collapsed particles in this sense is advantageous, since it is the direct evidence of the core-shell morphology. For the determination of morphology of particles with well-pronounced spherical shape other methods should be used.

### **Determination of particle morphology**

Toluene-containing polyamide particles showed mainly spherical shape (Fig. 2). Some particles were unintendedly broken on one of the preparation steps. Spherical PA core-shell particles were generally found to be very fragile and got broken even being handled with special precautions (very soft centrifugation regime, freeze-drying directly on the SEM sample holder). Therefore, it was concluded that polymeric shells were very fragile, which might be considered as disadvantage for the future possible application of such microparticulate systems. However, it was rather advantageous for the purpose of this study, since core-shell morphology could be easily ascertained. This morphology was observed for all types of PA microparticles prepared in this work independently of solvent used.

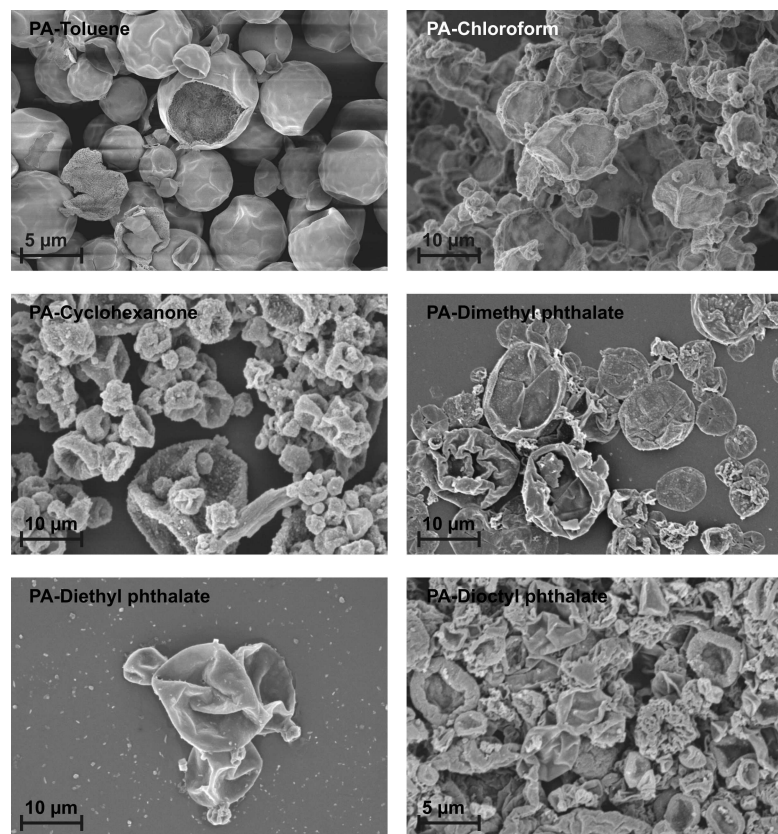


**Fig. 2.** SEM images of the PA microparticles.

Analysis of PU and PUa particle morphology was made on the basis of SEM of crushed particles. Application of TEM was not appropriate because of the comparatively big size of the particles and low contrast between polymeric shell and organic particle core. One should emphasize that distinction between the particle morphologies is not straightforward. For the sake of differentiation, only the particles having well-expressed solid shell and empty core will be called here as “core-shell”. If the polymer does not have any voids, the particles will be considered to be “compact”. Some particles possess morphologies lying between “compact” and “core-shell” with the polymer non-homogeneously distributed over the particle volume and forming some noticeable empty voids there. These microparticles were considered as possessing “multicompartment” morphology.

Particles containing toluene exhibit core-shell morphology in both PU (Fig. 3) and PUa (Fig. 4) cases. To establish this for PUa-toluene particles, crushing (or cutting) them was not necessary, since the particles were collapsed and their core-shell morphology could be deduced from the outer appearance.

The PU particles possess a lot of folds, but do not collapse even if they have a cavity inside. From the latter fact one can draw a conclusion about mechanical properties of particles: although SEM images reveal higher wall thickness for PUa particles, these walls are essentially softer than in the PU case.

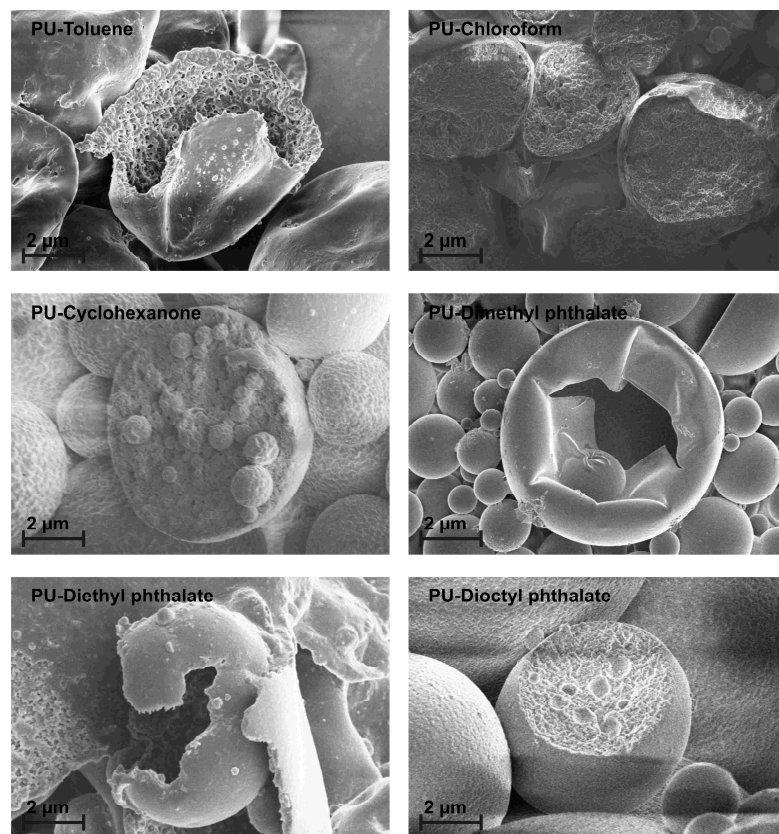


**Fig. 3.** SEM images of the crushed PU microparticles.

PU (Fig. 3) and PUa (Fig. 4) particles containing chloroform have different morphology. PU-chloroform particles consist of dense outer shell and “lumpy” core.

Even though the core and the shell parts can be distinguished in this case, this type of morphology will be considered as “compact”, since a significant part of the polymer is distributed inside the particle. PUa-chloroform particles also have some parts of polymer inside the cavity, but in this case the grains of polymers are easy to distinguish and the majority of the polymer is localized on the periphery of the particle, therefore the morphology of PUa-chloroform particles is considered to be of core-shell type.

PU (Fig. 3) and PUa (Fig. 4) particles containing cyclohexanone have slightly different morphology. PU-cyclohexanone particles have dense and homogeneous inner structure, while PUa-cyclohexanone ones show some signs of phase separation on the micro level. The polymer is homogeneously distributed over the inner particle volume, some smaller voids are however observable. These particles will be considered to possess multicompartiment morphology.

DMPH-containing particles (Fig. 3 and 4) made of PU and PUa differ significantly. PU-DMPH particles are mostly spherical, some (the biggest) have folds. PUa-DMPH particles are not collapsed, but have very irregular non-spherical shape with many folds on the surface.

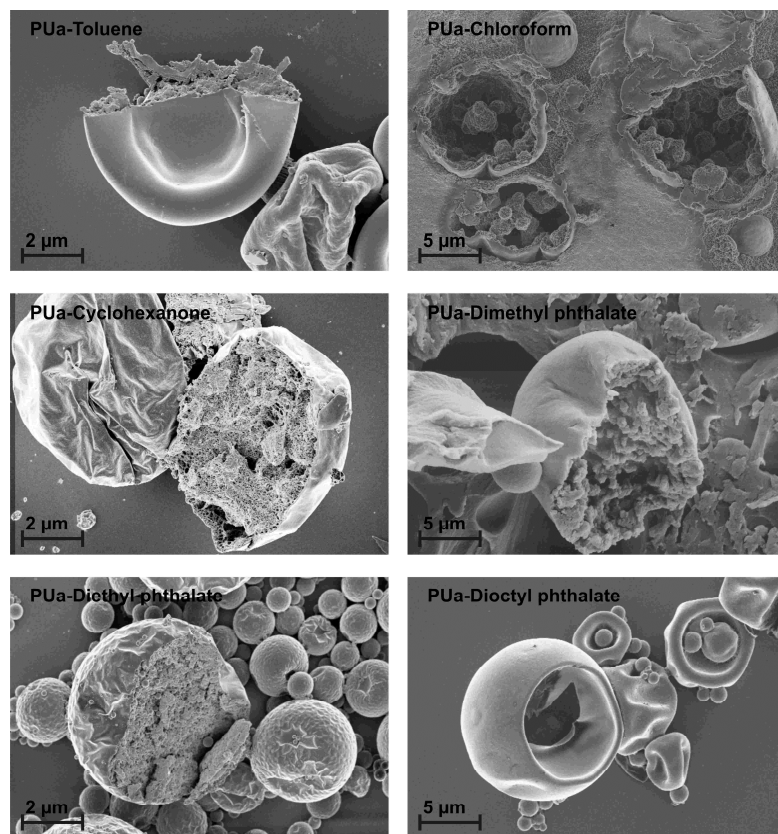


**Fig. 4.** SEM images of the crushed PUa microparticles.

PU-DMPH particles have core-shell morphology with comparatively thin and elastic shell. PUa-DMPH particles possess morphology similar to the PU-chloroform ones. According to our terminology these particles are compact, even distinction between the core and shell parts is possible.

PU-DEPh and PUa-DEPh particles (Fig. 3 and 4) look similar: generally spherical shape with many concavities and folds. The topography of the particle surface differs, but not significantly. The morphologies are, however, quite different: PU-DEPh particles are core-shell, while PUa-DEPh are compact. In contrast to PUa-DMPH particles, PUa-DEPh ones do not have any cavity inside; the polymer is homogeneously distributed over the particle volume.

DOPh-containing particles (Fig. 3 and 4) have different appearance. The surface of the PUa-DOPh particles is very smooth, many deep folds can be seen; some particles are collapsed. The surface of the PU-DOPh is rough. Particles differ in morphology as well: PU-DOPh particles have compact morphology; core and shell cannot be distinguished. PUa-DOPh particles demonstrate core-shell morphology with thin and elastic shells, very similar to the PU-DMPH particles.

From the analysis of outer appearance and morphology of the particles made of different solvent-polymer combinations one can conclude the following: neither spherical nor

irregular shape (with folds and concavities) of particles can be attributed to the particles morphology. Additional analysis such as TEM (which is not always useful) or SEM of crushed particles is always needed to draw conclusions on particle morphology. Appearance of completely collapsed polymeric particles alone can be considered as an evidence for their core-shell morphology.

For the 18 polymer-solvent combinations presented here, three general types of particle morphologies were observed: core-shell morphology with well-defined solid polymeric shell and core consisting of a solvent; compact morphology with polymer distributed homogeneously over the particle volume; multicompartiment morphology somehow in-between the ones described before: polymer is separated from the solvent in the form of grains, polymer grains are distributed within the particle volume either homogeneously or inhomogeneously. The polymer grains vary in size: for PUa-chloroform or PUa-DMPH particles the grains are easy to distinguish, while in some cases distinguishing between compact and multicompartiment morphologies is problematic (PU-chloroform and PUa-CH<sub>n</sub> particles).

The morphology of particles is not solvent- or polymer-specific, but it is specific for every polymer-solvent combination. The summary effect of the polymer-solvent interactions at certain particle composition (which can be expressed as solvent/polymer ratio) leads either to a phase separation between the two components or to their complete mixing. When the solvent-polymer interactions are thermodynamically favorable, solvent molecules will distribute homogeneously within the polymer matrix. Formation of compact morphology is therefore an analogue of the swelling, or plasticization, process.

The fact that the particles made of the same polymer prepared at the same conditions can be influenced so much by the solvent type is interesting by itself. But it would be even more interesting to find out, whether it is the consequence of the polymer-solvent interactions only (thermodynamically-dictated process) or kinetic factors are involved as well. In order to clarify this point, the extent of mutual affinity of each polymer/solvent pair should be estimated. For that, experiments on swelling of pre-formed individual polymers in a number of solvents have been carried out.

### **Swelling behavior of pure polymers and its correlation with particle morphology**

In order to find the correlation between particle morphology and polymer-solvent mutual affinities, swellability of pure polymers in a number of liquids has been investigated. For that, pure PU, PUa and PA polymers were additionally synthesized (see experimental

section). The swelling behavior of the three synthesized pure polymers in 18 different solvents was investigated. The solvents were: toluene, chloroform, cyclohexanone, dimethyl phthalate, diethyl phthalate, dioctyl phthalate, anise aldehyde, 2-methylbenzothiazole, tetrahydrofuran, styrene, N-methyl-2-Pyrrolidone, dimethyl sulfoxide, 1-dodecanethiol, 2,2,2-trifluoro ethanol, 1-hexanol, diaminocyclohexane, ethanol, methanol, acetone. The results of the swelling experiment are schematically represented in Fig. 5.

The first six solvents are the same as used for the preparation of 2-component particles and morphology determination experiments. The other twelve solvents were chosen in a manner to cover a broad variety of solvency properties, which were estimated on the basis of the Hansen solubility parameter values. The data on swelling in these solvents is essential for the further discussion. The values of HSP were taken from the HSP database available online [44].

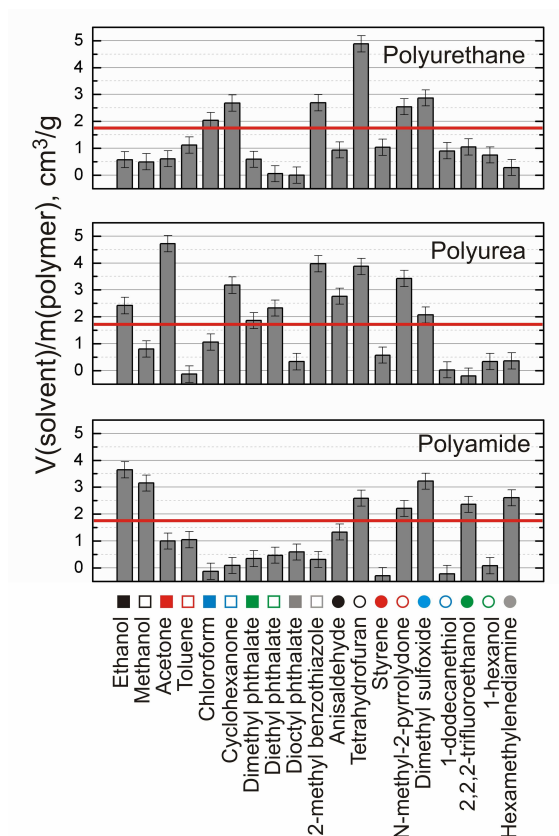


**Fig. 5.** Swellability of polymers in different solvents. The red line represents the “threshold extent of swelling”

In order to divide the solvents into two groups, namely “good” and “poor” ones, one should define an extent of swelling of polymer that a solvent has to cause in order to be considered as a good one. This would mean that interactions between the solvent and a polymer are thermodynamically favorable. For that Flory’s approach is a very useful one. Unfortunately, determination of interaction parameters for cross-linked polymers is not

straightforward, since it requires information on the crosslinking density of polymers, which is not easy to determine for micron-size objects.

To avoid this difficulty, we introduced an auxiliary parameter, that allowed the separation of all used solvents into two groups (“good” and “poor” solvents) and was useful for the further data analysis. The so called “threshold extent of swelling” expressed as volume of uptaken solvent divided by mass of polymer ( $\text{cm}^3/\text{g}$ ) is postulated to be equal to the ratio of solvent component volume to the mass of polymer component which was equal in all particle syntheses. Thus, if the whole volume of solvent present in each particle can be absorbed by a polymer and particles with compact morphology are formed as a result, this solvent is “good” and the equilibrium swellability provided by this solvent should be above the “threshold extent of swelling”. For the core-shell and multicompartment morphologies, the opposite should be valid: there is a certain extent of phase separation inside the particle, therefore the solvent can be considered to be a “poor” one and the equilibrium swellability should be below the “threshold extent of swelling”. If the latter is valid for each polymer/solvent pair, one can conclude that the morphology of microparticles is solely determined by polymer-solvent interactions, while other factors play only a minor role.

“Threshold extent of swelling” is a useful parameter, since it has basically the same value for each batch of prepared particles, because the initial ratio of components (v/wt) was constant in each experiment. According to the initial composition of oil droplets the threshold value of swelling in the present study can be roughly estimated as  $70/40 = 1.75 \text{ cm}^3/\text{g}$ . Therefore, if one gram of polymer was able to absorb more than 1.75 ml of solvent, the solvent could be considered as a “good” one, otherwise it was considered as “poor”. So, the terms “good solvent” and “poor solvent” are not used in the classical meaning and are not attributed to the classical Flory  $\chi$  interaction parameter [45].

Swelling behavior of pure polymers in most cases correlated with the morphology of the resulting particles. The particles, containing “good” solvent, exhibit compact architecture, while in case of poor solvent core-shell morphology is observed (Table 1). Only in two cases, the morphology of particles and the swelling behavior of the pure polymers do not correlate: for the pairs PU-DOPh and PUa-CHn.

The correlation between the swelling behavior of a polymer and the particle morphology was expected, since the morphology reflects the polymer-solvent phase behavior. The final state of the polymer-solvent mixture can be achieved by two different pathways:

- pre-formed polymer is brought into contact with a solvent. This pathway describes the swelling experiment.

- formation of the polymer happens in the presence of solvent. This pathway reflects the process of particle formation.

| Polymer/<br>solvent | PU                  |                                       | PUa                 |                                       | PA                  |                                       |
|---------------------|---------------------|---------------------------------------|---------------------|---------------------------------------|---------------------|---------------------------------------|
|                     | Compact morphology? | „good“ solvent (swelling experiment)? | Compact morphology? | „good“ solvent (swelling experiment)? | Compact morphology? | „good“ solvent (swelling experiment)? |
| Toluene             | -                   | -                                     | -                   | -                                     | -                   | -                                     |
| Chloroform          | +/-                 | +/-                                   | -                   | -                                     | -                   | -                                     |
| Cyclohexanone       | +                   | +                                     | +/-                 | +                                     | -                   | -                                     |
| Dimethylphthalate   | -                   | -                                     | +/-                 | +/-                                   | -                   | -                                     |
| Diethylphthalate    | -                   | -                                     | +                   | +                                     | -                   | -                                     |
| Dioctylphthalate    | +                   | -                                     | -                   | -                                     | -                   | -                                     |

**Table 1.** The “+” and “-” are positive and negative answers to the questions about particle morphology and solvent property, +/- stays for multicompartiment particles. If both answers are positive (or negative), a correlation between the swelling behavior and particle morphology is concluded; the pair of table cells corresponding to a certain polymer-solvent combination are marked green in this case. If the answers do not coincide the pair of cells is marked red.

The mismatch in swelling behavior of polymer and corresponding particle morphology for the PU-DOPh combination can be explained in a few ways. The simplest way is to assume, that the equilibrium was not achieved in the swelling experiment. It is known that the kinetics of polymer dissolution and/or swelling can be very slow due to extremely low mobility of the polymeric chains, especially for the cross-linked polymers. Some polymers being formally soluble need an extremely long time (sometimes years) in contact with the solvent to achieve equilibrium.

The other reason can be incomplete identity of the pure polymer and polymer from the particle due to the difference in the preparation conditions. Thus, polymers synthesized in different solvent might have different crosslinking density and conformation [46]. Both of these parameters can influence the swelling ability of polymers.

Another reason may result from the difficulty of distinguishing between the structures. In the present work, three possible morphologies are considered: core-shell, compact and multicompartiment. The distinction between the two latter ones is not trivial due to possible phase separation happening on the submicron- or nanolevel, which is non-observable by SEM. In this case, polymer would form a sponge-like structure with solvent distributed inside the pores. When the size of pores is small enough, they might be not visible by SEM; the

morphology can be attributed to the compact one, although phase separation on the microlevel has formally happened.

To conclude this section, one can say that in most of cases (16 out of 18), the morphology- and swelling-related experiments correlate. However, there are cases, when they don't. In many cases, when interfacial polymerization for encapsulation is utilized, it could be anticipated that, since the polymerization reaction happens directly on the boundary between the two immiscible phases, the formation of core-shell morphology could be always expected. Here, we have shown that it is generally incorrect and certain precautions have always to be made in order to achieve the desired structure.

### **Extension of Hansen solubility approach to the particle morphology**

The solubility sphere is another suitable way to present graphically the solubility/swelling behavior of polymers. For every given polymer, any solvent located inside the solubility sphere is considered as “good” one, while the ones outside are “poor”. Keeping in mind the correlation between particle morphology and swellability, one would expect that the solvents located inside the solubility sphere of a given polymer (“good” ones) should give compact particles, while the ones located outside (“poor” ones) should yield other (i.e. compact or multicompartiment) structures. To underline one more time, the latter is valid for all substances and not only for the ones where the swelling behavior was already tested.

The desired morphology of the particles is usually dictated by the application. Thus, morphology of microparticles is closely entwined with many important properties, such as, for example, release profile [26]. Usage of the approach presented here opens a broad range of new possibilities for the design of particles with desired properties in a comparatively easy fashion. When certain morphology of particles is required, the choice of core material can be made according to the solubility sphere of a polymer. It is also valid the other way around – the polymer with a certain solubility sphere should be chosen when the core material and the desired morphology are pre-conditioned. This is not a new idea; already in 1975 W. Sliwka [26] postulated that for obtaining core-shell particles with the shell impermeable to its liquid core material, Hildebrand parameters can be utilized. Since permeability of a capsule wall is closely related to solubility/swelling phenomena, the concept is basically the same. Advanced version of the morphology of nanocapsules on the basis of HSP approach was demonstrated a very short while ago by Landfester and co-workers [35]. Because the permeability of small molecules of encapsulated volatile compounds through the polymer shell is closely related to the solubility of the latter and finely to the solute-polymer interaction, it was possible to use

the HSP concept for the targeted synthesis of high diffusion-barrier nanocapsules containing highly volatile substances. The authors of Ref. [35] investigated a series of volatile fragrance-like compounds and showed that the most important parameter mainly responsible for the core-shell morphology of nanocapsules and barrier properties of their shell is  $\delta_H$ , HSP for hydrogen bonding. Moreover, a linear relationship between encapsulation efficiency and this parameter was observed allowing the prediction of the encapsulation efficiency of any material in the used acid-functionalized acrylic copolymer. In addition, correlation between volume fractions of the components of the mixed “oil” phase and corresponding  $\delta_H$  of these enables the increase of encapsulation efficiency of the poorly encapsulated materials by the simple addition of the mediating substances [35].

Once the solubility sphere of a polymer is constructed (Fig. 6), the solubility/swelling behavior can be extended to all possible substances with known HSP. Application of the HSP theory allows the prediction of polymer solubility/swelling for any given substance with known HSP parameters on the basis of a limited data set [40]. The latter makes the theory so attractive for applied chemistry and technology, since the choice of the system components is usually performed on the basis of a large number of different parameters that should mutually match. Even slight changes in the technology may lead to the necessity to find an analogue to a used solvent in the sense of solvency but carrying different chemistry. The HSP approach is indispensable for this kind of tasks.

Construction of a solubility sphere can be made on the basis either of swelling behavior of polymers or of available data on the particle morphology. As it was already shown above (Table 1), these two characteristics do almost always coincide. Therefore, relative simple swelling experiments allow quite precise prediction of the capsules morphology for three shell polymers used. However, if the final goal is the exact prediction of the morphology of particles to be prepared, the construction of the solubility sphere on the basis of the existing data on the particle morphology (when available) seems to be more reliable. In spite of the model character of different binary polymer-solvent systems used in this study some of them could be directly applied in the self-healing materials in a manner described by Caruso et al. [47] or Blaiszik et al. [16]. In the former case [47], the successful usage of solvents to heal cracks in thermoset materials at room temperature in an autonomic fashion was demonstrated where the solvent delivery to damaged site involved the fracture of embedded solvent filled microcapsules with the core-shell morphology. For particular solvents, the recovery grade by this autonomic self-healing system can reach up to 82% of the materials' original fracture toughness. The advanced version of this method was developed by Blaiszik et al. [16] where

the solutions of epoxy-based reactive sealing agents in “oil” soluble solvents were encapsulated in polymeric microcapsules with thin urea–formaldehyde shells and then successfully embedded into an epoxy matrix and ruptured by a propagating crack. After rupture, the formation an epoxy film was visible on the crack facet, manifesting the delivery of the reactive epoxy resin to the damage site and providing evidence and that capsules prepared by this method are suitable for use in self-healing materials.

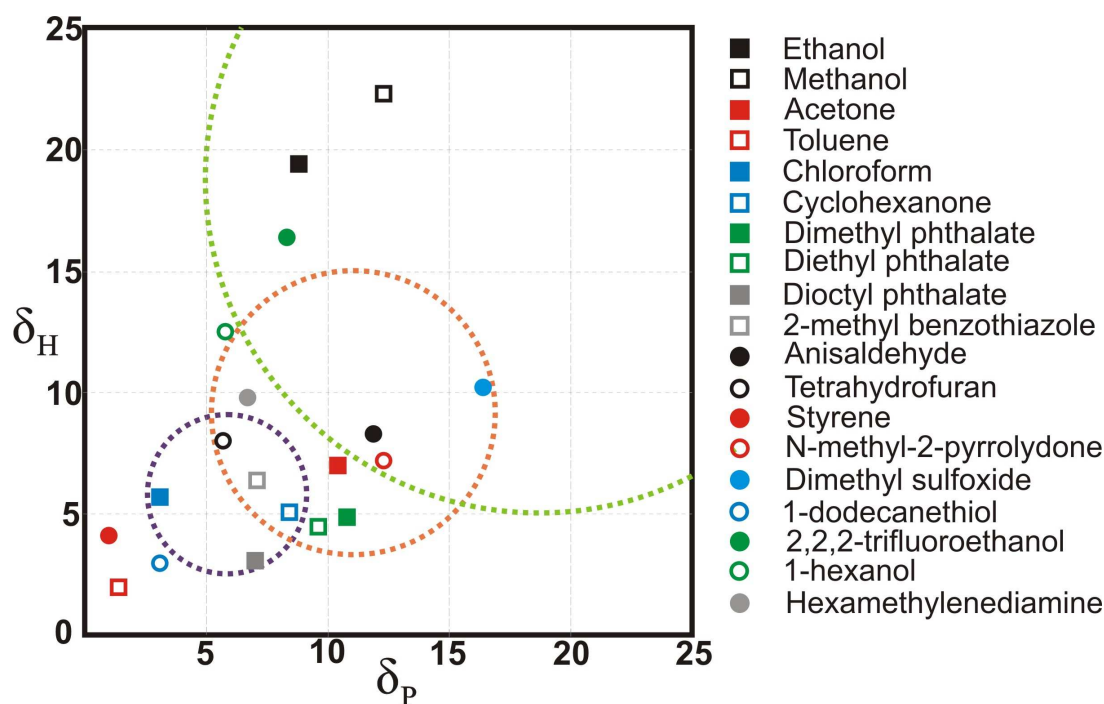


**Fig. 6.** Solubility spheres of PU (dark magenta border line), PUa (orange) and PA (green) experimentally determined based on the swelling experiments on the HSP graph  $\delta_H(\delta_P)$ .

### The mechanism

Based on the performed study, combined with the fundamental knowledge on the physical chemistry and phase behavior of polymers, one can postulate a common mechanism, leading to the formation of polymer particles with different morphology. Let us consider an individual droplet (see Fig. 7a) of solvent with dissolved monomer 1. This droplet is immersed into water solution of monomer 2. At the moment when these two phases come into contact, the polymerization reaction starts and the cross-linked polymer network begins to grow. Until a certain moment of time (percolation threshold or the point of gelation [48]) the system keeps a certain extent of mobility. The oligomers of relatively low molecular mass are not “attached” to each other and are free to diffuse; the molecules of the solvent are mobile, too.

In case the solvent is a “good” one, on the step of oligomer formation, a gradient of chemical potential of the solvent will appear between the center of the droplet (where the concentration of the polymer is close to zero) and the sphere surface (where the concentration of polymer or oligomers is relatively high). Due to this gradient a flow of “good” solvent towards the sphere surface will appear. An opposite flow of the oligomers will be directed towards the center of the droplet. Consequently, dilution of the polymer on the surface and an increase of polymer concentration in the center of the sphere occur. In an ideal case, after reaching the gelation point one would find an infinite network with solvent homogeneously distributed in the network, or a (micro)gel (Fig. 7a, right).

In case of a “poor” solvent, when the affinity between the polymer and the solvent is minimal, the “enthalpic” driving force of mixing of two types of molecules (oligomers and solvent) inside the sphere is absent; the oligomers will stay at the place they were formed, close to the droplet interface. The molecules of oil-soluble monomer (initially homogeneously distributed in the solvent), would diffuse towards the surface of the particle, where they are consumed due to the polymerization reaction. Finally, the concentration of the monomer close to the center of the particle will decrease with time and reach minimal value when the polymerization will be accomplished. As the result, one will find well-defined core-shell morphology with the core composed of solvent and the shell composed of the polymer (Fig. 7a, left).

In an intermediate case, the polymer could have certain affinity to the solvent, but not enough to absorb the whole available amount of solvent. In this case, one could obtain a core-shell particle, but the thickness of the shell will be higher compared to the previous case (zero affinity or no swelling of polymer, Fig. 7a, middle). In this case, polymer will still precipitate on the surface of the droplets forming a shell, but it will enclose certain part of the solvent. The higher the swelling ability of the polymer, the thicker shell will be formed, leading in the limit case to a shell thickness equal to the particle radius, or compact morphology, described in the beginning.

In the case of a “poor” solvent, the “non-entropic” driving force for the mixing of two types of molecules inside the sphere is absent. Nevertheless the presence of solvent on the surface of the droplet can be energetically favorable (solvent is more surface active than the forming oligomers or due to the entropic forces). In this case, solvent molecules will tend to concentrate on the droplet surface replacing the oligomers and leading to the formation of inverse core-shell structure (Fig. 7b, right).

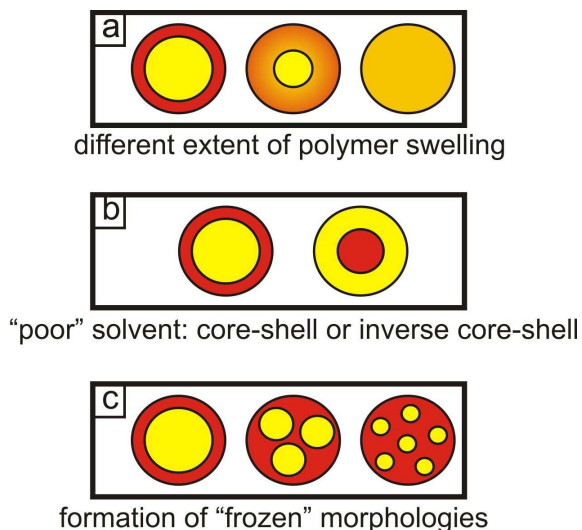


**Fig.7.** Possible particle morphologies for the two-component system solvent/cross-linked polymer. a) Gelation happens on the final stage of the polymerization reaction, the swellability of a polymer in a solvent determines the shell thickness. b) Gelation happens on the final stage of the polymerization reaction, final conformation is determined by surface tension forces. c) Gelation happens on one of the initial steps of the polymerization reaction. The size and the number of pores depend on the difference between the swelling abilities of the polymers with increasing molecular mass and degree of cross-linking.

All previously discussed scenarios are valid for the situation when gelation happens on the last stage of the polymerization. At the same time, for highly cross-linked polymeric networks, gelation might happen on the initial stages of polymerization. Proceeding polymerization reaction leads to the increase of the crosslinking density of the formed 3D network.

Generally, the swelling ability of the polymer decreases with the increase of polymer molecular mass and degree of cross-linking. Therefore, theoretically, a situation can appear when a certain solvent is still “good” for oligomers but is already “poor” for the polymer. In this case, the oligomers will diffuse to the droplet interior and undergo cross-linking there. After the gelation point is reached (polymer is homogeneously distributed over the droplet volume) the mobility of these polymer networks will be limited. The following increase of molar mass or/and degree of cross-linking can lead to the situation when the formed polymer is not “compatible” with the solvent anymore. The latter will induce shrinkage of the polymer network and release of the solvent in the existing cavities leading to the formation of porous or multicompartiment structures (Fig. 7c). The size and the number of pores will depend on the difference between the swelling abilities of the polymers with different molecular mass and degree of crosslinking.

## **Conclusions**

The approach presented here is general and can be applied to the whole spectrum of polymeric microobjects enclosing liquids. The idea, that the interactions between the components in a polymer composite determine their final structure, is far from being new. The message we would like to broadcast here is that keeping these interactions in mind is crucial for being able to tailor the properties of the designed systems. The processes of microgel formation, which we have chosen to illustrate the phenomena of spontaneous structuring on the microlevel, have a broad range of applications. At the same time, the chemistry involved is well studied and established, which allows making straightforward conclusions based on the data obtained. We hope that the suggested mechanism explaining formation of microobjects with defined morphologies will contribute to better understanding of similar and related systems, finally resulting in better control over systems' performance.

## **Acknowledgements**

D. Grigoriev acknowledges the financial support from the project “SigmaA” in the framework of “EXIST Transfer of Research program” of the Federal Ministry of Economics and Energy (BMWi), Germany.

## References

1. S. van der Zwaag, In: Self Healing Materials. An Alternative Approach to 20 Centuries of Materials Science, (Eds: S. van der Zwaag), Ch.1 An Introduction to Material Design Principles: Damage Prevention versus Damage Management Self Healing Materials, Springer, Dordrecht, The Netherlands, 2007, V. 100, 1-18.
2. S.K. Ghosh, In: Self-healing Materials: Fundamentals, Design Strategies, and Applications, (Eds: S. K. Ghosh), Ch.1 Self-healing Materials: Fundamentals, Design Strategies, and Applications, Wiley-VCH, Weinheim, Germany 2009, 1-28.
3. S. van der Zwaag, N.H. van Dijk, H.M. Jonkers, S.D. Mookhoek and W.G. Sloof, Self-healing behavior in man-made engineering materials: bioinspired but taking into account their intrinsic character, *Phil. Trans. R. Soc. A* 367 (2009) 1689-1704.
4. B.J. Blaiszik, S.L.B. Kramer, S.C. Olugebefola, J.S. Moore, N.R. Sottos, S.R. White, Self-Healing Polymers and Composites, *Annu. Rev. Mater. Res.* 40 (2010) 179-211.
5. M.D. Hager, P. Greil, C. Leyens, S. van der Zwaag, and U.S. Schubert, Self-Healing Materials, *Adv. Mater.* 22 (2010) 5424-5430.
6. R.S. Trask and I.P. Bond, Biomimetic self-healing of advanced composite structures using hollow glass fibres, *Smart Mater. Struct.* 15 (2006) 704-710.
7. K.S. Toohey, N.R. Sottos, J.A. Lewis, J.S. Moore, S.R. White, Self-healing materials with microvascular networks, *Nature Mater.* 6 (2007) 581-585.
8. C.J. Hansen, W. Wu, K.S. Toohey, N.R. Sottos, S.R. White, J.A. Lewis, Self-Healing Materials with Interpenetrating Microvascular Networks, *Adv. Mater.* 21 (2009) 4143-4147.
9. L.M. Bellan, S.P. Singh, P.W. Henderson, T.J. Porri, H.G. Craigheada and J.A. Spector, Fabrication of an artificial 3-dimensional vascular network using sacrificial sugar structures, *Soft Matter* 5 (2009) 1354-1357.
10. C.M. Dry, N.R. Sottos, Passive smart self-repair in polymer matrix composite materials. *Proc. SPIE* 1916 (1993) Smart Structures and Materials 1993: Smart Materials, 438-444.
11. C.M. Dry, Procedures developed for self-repair of polymer matrix composite materials", *Comp. Struct.* 3 (1996) 263-269.
12. S.R. White, N.R. Sottos, P.H. Geubelle, J.S. Moore, M.R. Kessler, S.R. Sriram, E.N. Brown & S. Viswanathan, Autonomic healing of polymer composites, *Nature* 409 (2001, 15 February) 794-797.
13. S.H. Cho, H.M. Andersson, S.R. White, N.R. Sottos, and P.V. Braun, Polydimethylsiloxane-Based Self-Healing Materials, *Adv. Mater.* 18 (2006) 997-1000.

14. J. Yang, M.W. Keller, J.S. Moore, S.R. White, and N.R. Sottos, Microencapsulation of Isocyanates for Self-Healing Polymers, *Macromolecules* 41 (2008) 9650-9655.
15. B.J. Blaiszik, N.R. Sottos, S.R. White, Nanocapsules for self-healing materials, *Compos. Sci. Technol.* 68 (2008) 978-986.
16. B.J. Blaiszik, M.M. Caruso, D.A. McIlroy, J.S. Moore, S.R. White, N.R. Sottos, Microcapsules filled with reactive solutions for self-healing materials, *Polymer* 50 (2009) 990-997.
17. Y. Zhao, J. Fickert, K. Landfester, and D. Crespy, Encapsulation of Self-Healing Agents in Polymer Nanocapsules, *Small* 8 (2012) 2954-2958.
18. A.P. Esser-Kahn, S.A. Odom, N.R. Sottos, S.R. White, and J.S. Moore, Triggered Release from Polymer Capsules, *Macromolecules* 44 (2011) 5539-5553.
19. A. Kumar, L.D. Stephenson, J.N. Murray, Self-healing coatings for steel, *Prog. Org. Coat.* 55 (2006) 244-253.
20. C. Suryanarayana, K.C. Rao, D. Kumar, Preparation and characterization of microcapsules containing linseed oil and its use in self-healing coatings, *Prog. Org. Coat.* 63 (2008) 72-78.
21. S.H. Cho, S.R. White, and P.V. Braun, Self-Healing Polymer Coatings, *Adv. Mater.* 21 (2009) 645-649.
22. A.E. Hughes, I.S. Cole, T.H. Muster and R.J. Varley, Designing green, self-healing coatings for metal protection, *NPG Asia Mater.* 2 (2010) 142-151.
23. A. Latnikova, D.O. Grigoriev, J. Hartmann, H. Möhwald and D.G. Shchukin, Polyfunctional active coatings with damage-triggered water-repelling effect, *Soft Matter* 7 (2011) 369-372.
24. D.G. Shchukin, Container-based multifunctional self-healing polymer coatings, *Polymer Chemistry* 4 (2013) 4871-4877.
25. D.O. Grigoriev, M.F. Haase, N. Fandrich, A. Latnikova, D.G. Shchukin, Emulsion route in fabrication of micro and nanocontainers for biomimetic self-healing and self-protecting functional coatings, *Bioinspir. Biomim. Nanobiomater* 1 (2012) 101-116.
26. W. Sliwka, Microencapsulation, *Angew. Chem. Int. Ed.* 14 (1975) 539-550.
27. D. Crespy, M. Stark, C. Hoffmann-Richter, U. Ziener, and K. Landfester, Polymeric Nanoreactors for Hydrophilic Reagents Synthesized by Interfacial Polycondensation on Miniemulsion Droplets, *Macromolecules* 40 (2007) 3122-3135.
28. K. Landfester, Miniemulsion Polymerization and the Structure of Polymer and Hybrid Nanoparticles, *Angew. Chem. Int. Ed.* 48 (2009) 4488-4507.

29. C.K. Weiss and K. Landfester, Miniemulsion Polymerization as a Means to Encapsulate Organic and Inorganic Materials, *Adv. Polym. Sci.* 233 (2010) 185-236.
30. D. Crespy and K. Landfester, Making dry fertile: a practical tour of non-aqueous emulsions and miniemulsions, their preparation and some applications, *Soft Matter* 7 (2011) 11054-11064.
31. Y. Zhao, D. Döhler, L.-P. Lv, W.H. Binder, K. Landfester, D. Crespy, Facile Phase-Separation Approach to Encapsulate Functionalized Polymers in Core-Shell Nanoparticles, *Macromol. Chem. Phys.* 215 (2014) 198-204.
32. I. Hofmeister, K. Landfester, and A. Taden, pH-Sensitive Nanocapsules with Barrier Properties: Fragrance Encapsulation and Controlled Release, *Macromolecules* 47 (2014) 5768-5773.
33. A. Latnikova, Polymeric capsules for self-healing anticorrosion coatings, PhD thesis, Potsdam University, Potsdam, Germany, 2012. Accessible online at the Institutional Repository of the University of Potsdam: <http://opus.kobv.de/ubp/volltexte/2012/6043/>
34. A. Latnikova, D.O. Grigoriev, H. Möhwald, and D.G. Shchukin, Capsules Made of Cross-Linked Polymers and Liquid Core: Possible Morphologies and Their Estimation on the Basis of Hansen Solubility Parameters, *J. Phys. Chem. C* 116 (2012) 8181-8187.
35. I. Hofmeister, K. Landfester, and A. Taden, Controlled Formation of Polymer Nanocapsules with High Diffusion-Barrier Properties and Prediction of Encapsulation Efficiency, *Angew. Chem. Int. Ed.* 54 (2015) 327-330.
36. C.M. Hansen, The Three Dimensional Solubility Parameter – Key to Paint Component Affinities I. Solvents, Plasticizers, Polymers, and Resins, *J. Paint Techn.* 39 (1967) 104-117.
37. C.M. Hansen, The Three Dimensional Solubility Parameter – Key to Paint Component Affinities II. Dyes, Emulsifiers, Mutual Solubility and Compatibility, and Pigments, *J. Paint Techn.* 39 (1967) 505-510.
38. C.M. Hansen, and K. Skaarup, The Three Dimensional Solubility Parameter – Key to Paint Component Affinities III. Independent Calculation of the Parameter Components, *J. Paint Techn.* 39 (1967) 511-514.
39. C.M. Hansen, Doctoral Dissertation, The Three Dimensional Solubility Parameter and Solvent Diffusion Coefficient, Their Importance in Surface Coating Formulation, Danish Technical Press, Copenhagen, 1967.
40. C.M. Hansen, Hansen Solubility Parameters: A User's Handbook, Second Ed. CRC Press, Boca Raton, FL, 2007.

41. M. Antonietti, and K. Landfester, Polyreactions in miniemulsions, *Prog. Polym. Sci.* 27 (2002) 689-757.
42. K. Landfester, Polyreactions in miniemulsions, *Macromol. Rapid Comm.* 22 (2001) 896-936.
43. R. Dubey, T.C. Shami, K.U. Bhasker Rao, H. Yoon, and V.K. Varadan, Synthesis of polyamide microcapsules and effect of critical point drying on physical aspect, *Smart Mater. Struct.* 18 (2009) 025021 (6 pp).
44. <http://www.hansen-solubility.com>
45. P.J. Flory, Phase equilibria in solutions of rod-like particles, *P. Roy. Soc. Lond. A Mat.* 234 (1956) 73-89.
46. P.J. Flory, and J. Rehner, Statistical mechanics of cross-linked polymer networks II. Swelling, *J. Chem. Phys.* 11 (1943) 521-526.
47. M.M. Caruso, D.A. Delafuente, V. Ho, N.R. Sottos, J.S. Moore, and S.R. White, Solvent-Promoted Self-Healing Epoxy Materials, *Macromolecules* 40 (2007) 8830-8832.
48. P.J. Flory, Molecular size distribution in three dimensional polymers. I. Gelation, *J. Am. Chem. Soc.* 63 (1941) 3083-3090.

## Table(s)

Table 1. The “+” and “-” are positive and negative answers to the questions about particle morphology and solvent property, +/- stays for multicompartement particles. If both answers are positive (or negative), a correlation between the swelling behavior and particle morphology is concluded; the pair of table cells corresponding to a certain polymer-solvent combination are marked green in this case. If the answers do not coincide the pair of cells is marked red.

## Figure legends

Figure 1. Left: Schematic representation of the interfacial polymerization process: two immiscible phases (A), emulsion formation (B), Second reactive monomer addition (C), monomer consumption leading to polymer particles formation (D). Right: Chemical reactions corresponding to the formation of urethane, urea and amide linkage.

Figure 2. SEM images of the PA microparticles.

Figure 3. SEM images of the crushed PU microparticles.

Figure 4. SEM images of the crushed PUa microparticles.

Figure 5. Swellability of polymers in different solvents. The red line represents the “threshold extent of swelling”.

Figure 6. Solubility spheres of PU (dark magenta border line), PUa (orange) and PA (green) experimentally determined based on the swelling experiments on the HSP graph  $\delta_H(\delta_D)$ .

Figure 7. Possible particle morphologies for the two-component system solvent/cross-linked polymer. a). Gelation happens on the final stage of the polymerization reaction, the swellability of a polymer in a solvent determines the shell thickness. b). Gelation happens on the final stage of the polymerization reaction, final conformation is determined by surface tension forces. c). Gelation happens on one of the initial steps of the polymerization reaction. The size and the number of pores depend on the difference between the swelling abilities of the polymers with increasing molecular mass and degree of cross-linking.